Longitudinal Field Modes Probed by Single Molecules

L. Novotny,* M. R. Beversluis, K. S. Youngworth, and T. G. Brown

The Institute of Optics, University of Rochester, Rochester, New York 14627
(Received 27 February 2001)

We demonstrate that a strong longitudinal, nonpropagating field is generated at the focus of a radially polarized beam mode. This field is localized in space and its energy density exceeds the energy density of the transverse field by more than a factor of 2. Single molecules with fixed absorption dipole moments are used to probe the longitudinal field. Vice versa, it is demonstrated that orientations of single molecules are efficiently mapped out in three dimensions by using a radially polarized beam as the excitation source. We also show that there is no momentum or energy transport associated with the longitudinal field.

Laser modes which exhibit a longitudinal electric field at the center of a focal region (longitudinal field modes) were proposed for several applications. For example, it was suggested that longitudinal modes could be used to accelerate a charged particle to high energies [1]. In this type of linear accelerator, a single optical beam can provide acceleration, focusing, and bunching of particles [2]. Longitudinal field modes were also proposed for the probing of absorption dipole moments of single molecules [3]. In fact, an excitation scheme which allows for an efficient orientation determination of single molecules is of importance for the study of single molecule kinetics and dynamics [4]. Single molecule orientation measurements are important for precise distance measurements using single-pair fluorescence resonant energy transfer [5], for monitoring rotational diffusion [6] and for studying conformational changes. Longitudinal field modes were also proposed for high resolution near-field optical microscopy [7]. In this scheme, the longitudinal field mode excites a strongly enhanced field at the end of a metal tip. Bringing the tip close to a sample surface allows for a localized optical interaction [8]. Recently, both longitudinal field modes and their azimuthal counterparts were introduced in confocal microscopy, and it has been demonstrated that these modes provide high sensitivity to surface gradients [9]. The early theoretical investigations used first order paraxial theory to estimate the longitudinal field strength [1]. More accurate results were obtained by using an angular spectrum representation for the focused field [9,10]. However, to our knowledge, no direct experimental measurements of the longitudinal field have been performed so far.

Mathematically, longitudinal field modes are generated by spatial derivatives of the fundamental laser mode [11]. The particular type of longitudinal mode depends on the mathematical form of the fundamental mode (Gaussian beam, Bessel beam) and on the coordinates which are being differentiated. For example, Hermite-Gaussian modes are generated by differentiation of the fundamental Gaussian beam with respect to Cartesian coordinates. A particularly strong longitudinal field is generated in the focus of a radially polarized mode. This type of mode can be gen-

erated by the superposition of two linearly polarized longitudinal field modes [9,12].

In this Letter we provide experimental measurements of the field distribution near the focus of a strongly focused radially polarized field mode. The fluorescence of single molecules with fixed absorption dipole orientation are used as probes for the local field distribution. Vice versa, a radially polarized beam can be used to accurately determine the three-dimensional orientation of the molecular absorption dipole moment. We find that the longitudinal field strength exceeds the strength of the transverse field by more than a factor of 2. The experimental data is in excellent agreement with rigorous theoretical calculations. We show that the longitudinal fields in the focal region do not propagate. Instead, they form a "reservoir" of electric energy density. Thus, similar to a standing wave, there is no net momentum associated with the photons in the focus of a longitudinal mode.

Our experimental setup is shown in Fig. 1. The fundamental laser mode of an Ar^+ laser ($\lambda = 488$ nm) is converted into two perpendicularly polarized Hermite-Gaussian $(1,0)$ modes which are then recombined to form
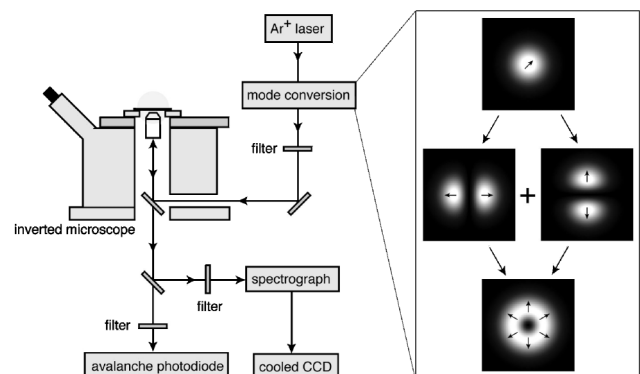

FIG. 1. Experimental setup: The fundamental laser mode of an Ar^+ laser ($\lambda = 488$ nm) is converted into a radially polarized mode and focused on a dielectic sample consisting of a PMMA layer with embedded dye molecules. The strength of the longitudinal field at the laser focus is determined by scanning individual molecules with fixed absorption dipole orientation through the laser focus and monitoring the fluorescence emission rate.

a radially polarized mode. The radially polarized beam is expanded and directed into an inverted microscope. A 45° dichroic filter reflects the beam upwards, and a high numerical aperture (NA = 1.4) objective focuses the beam on the sample surface. The sample is supported by a transparent glass cover slip and consists of individual $5,5'$-Ph$_2$-DiOC$_{18}$(3) molecules embedded in a PMMA film with a thickness of 10–30 nm. The molecules have a flat structure and are roughly 2.5 nm in length. To first order, the fluorescence rate R of an individual molecule near the laser focus is given by

$$R(\mathbf{r}) = c|\mathbf{d} \cdot \mathbf{E}(\mathbf{r})|^2, \tag{1}$$

where $\mathbf{d}$ is the unit vector along the absorption dipole moment of the molecule and $\mathbf{E}(\mathbf{r})$ is the complex electric field vector of the focused laser beam. The constant c is determined by the molecule's absorption cross section and quantum yield. The maximum fluorescence rate is limited by the triplet state lifetime and the intersystem crossing rate. A molecule preferentially emits into the medium of higher refractive index. Therefore, by using the same objective lens for detection as for excitation, we collect more than 50% of the emitted fluorescence photons. Taking into account the transmission properties of our filters and optical elements, as well as the quantum efficiency of the detector, we estimate the overall detection efficiency to be 25%–30%.

It has been shown that the field of a fundamental laser mode can be suitably filtered in order to provide comparable excitation strengths for different dipole orientations [4]. Such a filtered laser beam provides a means to spatially map out the dipole orientations of individual molecules. In this experiment, the excitation field $\mathbf{E}$ corresponds to the field of a radially polarized beam focused on the surface of a dielectric medium with a refractive index of $n = 1.52$. In a homogeneous medium, the focused field $\mathbf{E}^0$ of a radial beam mode can be written as an angular spectrum of plane waves similar to the work by Richards and Wolf [9,13]. By using cylindrical coordinates $\mathbf{r} = (\rho, \phi, z)$ and cylindrical vector components $\mathbf{E}^0 = (E_\rho^0, 0, E_z^0)$, we obtain

$$E_\rho^0(\mathbf{r}) = E_0 \int_0^{\theta_{max}} f_w(\theta)(\cos\theta)^{3/2}$$
$$\times \sin^2\theta J_1(k\rho\sin\theta)e^{ikz\cos\theta} \, d\theta, \tag{2}$$

$$E_z^0(\mathbf{r}) = E_0 \int_0^{\theta_{max}} f_w(\theta)(\cos\theta)^{1/2}$$
$$\times \sin^3\theta J_0(k\rho\sin\theta)e^{ikz\cos\theta} \, d\theta. \tag{3}$$

Here, the angle θ denotes the angle of a particular plane wave component with respect to the optical axis. The wave number k is equal to $k = n2\pi/\lambda$. θ_{max} is related to the numerical aperture by NA $= n\sin\theta_{max}$ and E_0 is a constant electric field amplitude. We choose an apodization

function $f_w(\theta)$ given by

$$f_w(\theta) = \exp\left[-\frac{1}{f_0^2}\frac{\sin^2\theta}{\sin^2\theta_{max}}\right], \tag{4}$$

where the parameter f_0 is the filling factor of the back-aperture of the objective. In terms of the beam waist w_0 of the primary beam, the focal length f, and the angle θ_{max}, it can be written as

$$f_0 = \frac{w_0}{f\sin\theta_{max}}. \tag{5}$$

For a completely overfilled backaperture $f_0 \to \infty$ and, consequently, $f_w(\theta) = 1$. In our experiments we use a filling factor of $f_0 = 1$.

The excitation field $\mathbf{E}$ in Eq. (1) is determined by the incident field $\mathbf{E}^0$ and the scattered field from the interface. The latter is calculated by applying the Fresnel reflection and transmission coefficients to each individual plane wave component. Figure 2A shows the resulting field strength E^2 as a function of the radial coordinate ρ in a plane 2 nm beneath the interface. Also shown are the strengths of the transverse field (E_ρ^2) and the longitudinal field (E_z^2). The former is characterized by two off-axis lobes, whereas the latter has a distinct peak on the optical axis. Surprisingly, the longitudinal field strength exceeds the transverse field strength by more than a factor of 2. This factor can be further increased by using a higher NA.

In order to experimentally verify the calculated longitudinal field strength we scan single molecules with fixed dipole orientation through the laser focus. A raster scan image is generated by recording the fluorescence rate R as a function of the lateral coordinate $\mathbf{r} = (x, y)$. Figures 2B–2E show calculated images for different molecular orientations. A molecule with its dipole transverse to the beam axis is excited only by the transverse field E_ρ. Therefore, the resulting image consists of two lobes aligned in the direction of the dipole moment (Fig. 2B). On the other hand, a molecule with its dipole in the direction of the beam axis is probed only by the longitudinal field E_z, and the resulting image has a single lobe at the center (Fig. 2E). Dipole orientations which have both transverse and longitudinal components render an image with two lobes but with one lobe more intense than the other (Figs. 2C and 2D). Once the excitation field is experimentally verified, the orientation of an arbitrary molecular absorption dipole can be efficiently determined based on the generated fluorescence image. In a first experiment, molecules were deposited on the surface of a glass cover slip and overcoated by a thin PMMA layer. In this case, all dipole moments are transverse to the optical axis and only patterns such as Fig. 2B are generated. Figure 3A confirms this expectation. The lobes corresponding to a single molecule are equal in intensity but the intensity varies from molecule to molecule (cf. molecules b and d). This is an indication that the local environment affects a molecule's absorption cross section and quantum yield. The image
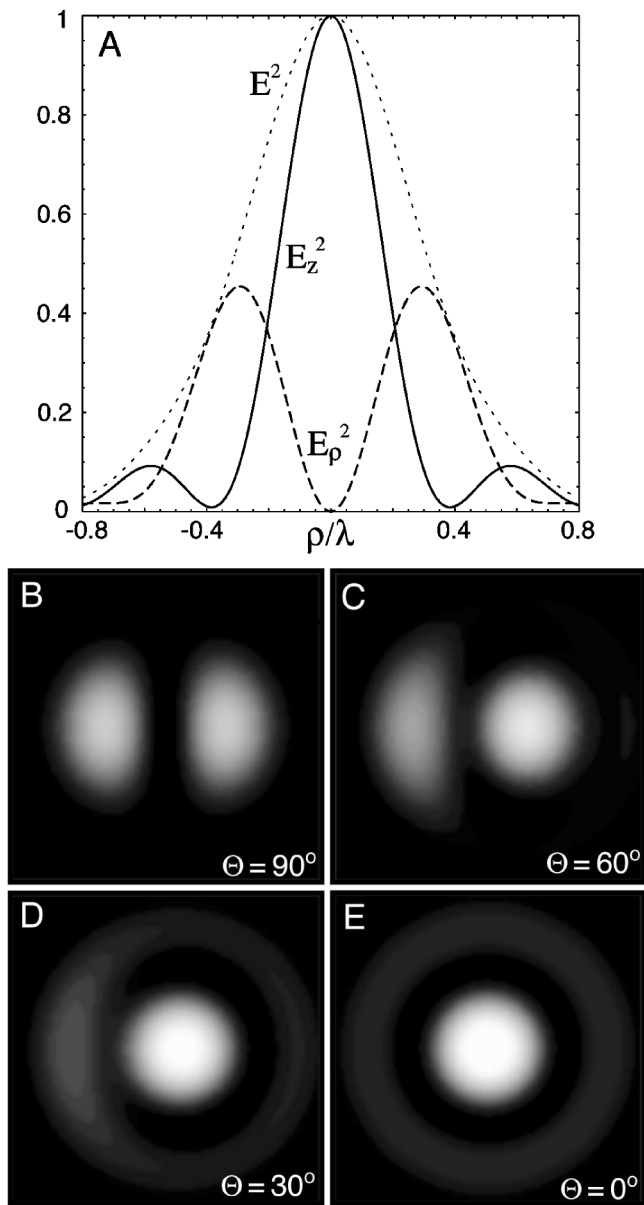
FIG. 2. (A) Comparison of longitudinal field strength E_z^2, transverse field strength E_ρ^2, and total field strength E^2 as a function of radial coordinate, evaluated 2 nm beneath the interface. (B)–(E) Calculated emission rate images $[R(x,y)]$ for different polar orientations of a molecule in the x-z plane. θ denotes the angle between the dipole axis and the beam axis.

of the molecule beside molecule a is truncated because of photobleaching during image acquisition. Molecules b and c are separated by less than a wavelength and their dipoles are at right angles to each other. Immediately after recording the image, a second image was acquired with a focused fundamental beam mode as the excitation source. This beam is polarized along the direction of the arrow in Fig. 3B. Molecules a and b are not excited because their dipoles are at right angles to the polarization, confirming that the absorption dipole of these molecules is oriented in the direction of the two lobes shown in Fig. 3A.
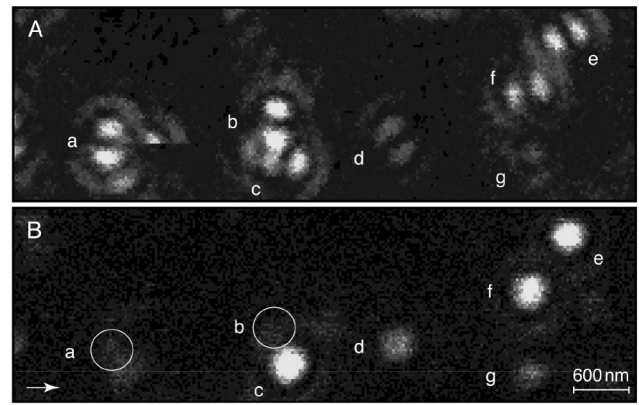

FIG. 3. Fluorescence rate images $[R(x,y)]$ of molecules oriented transverse to the beam axis. (A) Excitation with a focused radially polarized beam. Adjacent lobes define the direction of the molecular absorption dipole (cf. Fig. 2B). (B) Excitation with a focused fundamental Gaussian beam polarized in the direction of the arrow. Molecules a and b are not excited because their absorption dipole is perpendicular to the polarization.

In the next experiment, the dye molecules were intermixed with the PMMA solution. After spin deposition, the molecules were randomly oriented inside the PMMA layer. The fluorescence images should therefore render any of the patterns shown in Figs. 2B–2E. As shown in Fig. 4 these patterns are indeed measured. Molecule a has a dipole moment which is almost oriented along the beam axis. The two weak side lobes suggest an orientation of $10° < \theta < 30°$ (cf. Fig. 2D). A molecule with pure longitudinal dipole orientation ($\theta = 0°$) would render a symmetric outer ring (cf. Fig. 2E). Molecules b and e render a double-lobed pattern with one lobe clearly stronger than the other. The dipole orientation is roughly $\theta \approx 60°$. The dipole of the two remaining molecules c and d is almost purely transverse to the beam axis ($\theta \approx 90°$). The pattern of molecule d appears slightly distorted because it is

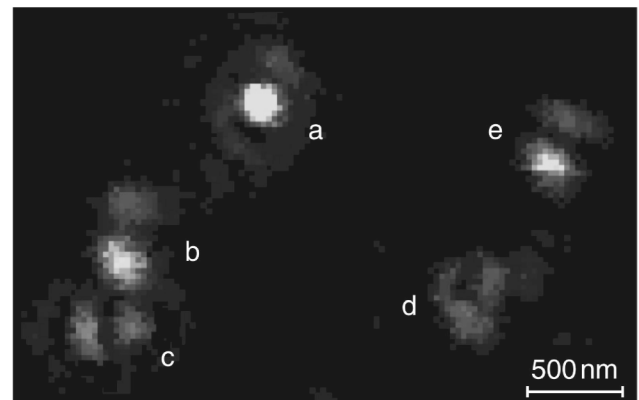

FIG. 4. Fluorescence rate images $[R(x,y)]$ of arbitrarily oriented molecules excited with a focused radially polarized beam. The dipole moment of molecule a is nearly longitudinal (cf. Fig. 2D), whereas the dipole moments of molecules c and d are transverse. Molecules b and e have an orientation of $\theta \approx 60°$ (cf. Fig. 2C).
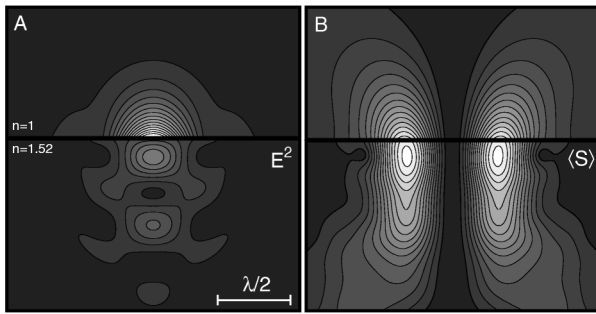
FIG. 5. (A) Electric field strength E^2 and (B) absolute value of the time averaged Poynting vector $\langle S \rangle$ of a radially polarized beam focused upward on the surface of a dielectric medium ($n = 1.52$). The longitudinal field E_z^2 centered on the beam axis does not propagate. Energy transport is associated only with the transverse field E_ρ^2.

overlayed with a faint background signal originating from an underlying molecule. Nevertheless, the overall intensity of the double-lobed pattern of molecules c and d is clearly weaker than the intensity of the other molecules. This suggests that the longitudinal field is indeed more intense than the transverse field. Because of molecular variations in absorption cross section and quantum yield, the longitudinal field strength has to be quantified by averaging over many molecules. We evaluated the patterns of many sample sections and determined that the ratio between longitudinal and transverse field is $(E_z^2 / E_\rho^2) \approx 2-3$. This number is in agreement with our previous calculations shown in Fig. 2A.

It is important to notice that the longitudinal field does *not* propagate. Since the magnetic field strength is zero along the optical axis [9], there is no energy transport at the center of the beam. Figure 5 shows the calculated electric field strength E^2 and the strength of the time averaged Poynting vector $\langle S \rangle$ in a plane containing the optical axis. At the center of the beam, E^2 has a maximum whereas $\langle S \rangle$ is zero. This demonstrates that energy transport and field momentum are associated only with the transverse field. It is remarkable that a longitudinal nonpropagating field can be generated by a propagating beam. Although there is an obvious analogy to a standing wave generated by counter-propagating plane waves, the nonpropagating field in the present situation is longitudinal and localized in space. As seen in Fig. 5, the interface does not significantly affect

the Poynting vector, whereas it greatly distorts the electric field strength. Because of the boundary conditions at the interface, the longitudinal field is discontinuous. The field strength is maximized just above the dielectric surface. This might be important in imaging and data storage applications based on solid immersion lenses. It must be emphasized that the generation of the nonpropagating, longitudinal field is independent of the presence of the interface. In our studies, the interface has been included in order to have an accurate comparison with experimental measurements. Finally, it should be noticed that the azimuthally polarized mode [9,14] is the magnetic analog of the radially polarized mode. Instead of a longitudinal electric field, the azimuthal beam has a longitudinal magnetic field at the focus. This type of beam may therefore be used to probe magnetic transitions in matter.

---

*Electronic address: novotny@optics.rochester.edu
[1] M. O. Scully, Appl. Phys. B **51**, 238 (1990).
[2] E. J. Bochove, G. T. Moore, and M. O. Scully, Phys. Rev. A **46**, 6640 (1992).
[3] J. J. Macklin *et al.*, Science **272**, 255 (1996).
[4] B. Sick, B. Hecht, and L. Novotny, Phys. Rev. Lett. **85**, 4482 (2000).
[5] T. Ha *et al.*, Proc. Natl. Acad. Sci. U.S.A. **93**, 6264 (1996).
[6] T. Ha *et al.*, Phys. Rev. Lett. **80**, 2093 (1998).
[7] L. Novotny, E. J. Sanchez, and X. S. Xie, Ultramicroscopy **71**, 21 (1998).
[8] E. J. Sanchez, L. Novotny, and X. S. Xie, Phys. Rev. Lett. **82**, 4014 (1999).
[9] K. S. Youngworth and T. G. Brown, Opt. Express **7**, 77 (2000).
[10] S. Quabis *et al.*, Appl. Phys. B **72**, 109 (2001).
[11] E. Zauderer, J. Opt. Soc. Am. A **3**, 465 (1986).
[12] S. C. Tidwell, D. H. Ford, and W. D. Kimura, Appl. Opt. **29**, 2234 (1990).
[13] B. Richards and E. Wolf, Proc. R. Soc. London A **253**, 358 (1959).
[14] D. G. Hall, Opt. Lett. **21**, 9 (1996).